Pulse-density-modulated power control of a 4 kW, 450 kHz voltage-source inverter for induction melting applications

Hideaki Fujita*   Hirofumi Akagi†
K. Sano‡   R. H. Leonard**

*Okayama University

†Okayama University

‡Sekisui Chemical Corporation Limited

**J. F. Jelenko & Corporation

Pulse Density Modulation Based Power Control of a 4kW 400kHz Voltage-Source Inverter for Induction Heating Applications

H. Fujita, H. Akagi   K. Sano, K. Mita   R. H. Leonard

Okayama University   Sekisui Chemical Co., Ltd.   J. F. Jelenko & Co.

Okayama, JAPAN   Kyoto, JAPAN   N.Y., U.S.A.

Abstract— This paper presents a 4kW 400kHz voltage-source inverter for induction heating applications, which is characterized by the power control based on PDM (Pulse Density Modulation). The pulse density modulated inverter makes an induction heating system simple and compact, thus leading to higher efficiency. The modulation strategy is proposed to realize an induction heating system capable of operation at the frequency and power level of interest. Some experimental results are shown to verify the validity of the concept.

I. INTRODUCTION

With remarkable progress in switching speed and capacity of MOSFET's and SIT's, voltage- or current-source inverters capable of operation at the output frequency of over 100kHz have been researched and developed for induction heating applications such as melting and surface quenching[1]~[4]. A high-frequency voltage-source inverter, however, has no ability to control the output power by itself, so that the output power of such an inverter has to be controlled by adjusting the dc input voltage. A thyristor bridge rectifier having a dc capacitor and reactor has been conventionally used as a variable dc-voltage power supply. This causes some problems in size and cost of induction heating systems.

In order to overcome the problems of the thyristor bridge rectifier, the following control schemes have been proposed with the focus on the use of a diode bridge rectifier as a dc power supply:

- frequency control based power control [5][6],

- pulse width modulation based power control [7],

- duty control based power control [8].

These control schemes, however, may result in an increase of switching losses and electromagnetic noises because it is impossible for switching devices such as MOSFET's and SIT's to be always turned on and off at zero current.

This paper describes an induction heating system of 4kW 400kHz, which is developed for dental casting machines.

The induction heating system consists of a single-phase diode rectifier, a single-phase voltage-source inverter using four MOSFET's and a series resonant circuit with a matching transformer. The output power control based on PDM enables us to use the diode rectifier as a dc power supply. Zero current switching is performed in a wide range from 80W to 3.6kW, reducing switching losses and improving efficiency. Moreover, the diode bridge rectifier having no dielectric capacitor on the dc side plays an important role in shaping the line current of the rectifier into sinusoid and unity power factor. Experimental waveforms, along with the analysis leading to the design, are included to verify the validity of the theory presented in this paper.

II. SYSTEM COFIGURATION

Fig.1 shows a system configuration of the induction heating system developed in this paper. The power circuit of the high-frequency inverter consists of a single-phase voltage-source inverter using four MOSFET's (2SK1521, Hitachi). The voltage rating of the MOSFET is 450V, and the current one is 50A. The loss-less snubber circuit consisting of only a small capacitor of 2000pF in each leg is connected between the drain and source of the MOSFET. The output of the inverter is connected to the series resonant circuit by a matching transformer with turn-ratio of 8:1.

The dc power supply for the inverter is a single-phase diode bridge rectifier in which no dc smoothing capacitor or reactor is connected except for a high frequency capacitor of $0.47\mu F$. This makes a great contribution to shaping the line current of the rectifier into sinusoid and unity power factor, because the inverter is seen as a pure resistor in the relationship between the dc voltage and current. The output power of the inverter varies at 120Hz, that is, twice as high as the line frequency of 60Hz, but such a variation of the output power does not cause any problem in melting.

III. PDM OPERATION

A. Principle of PDM operation

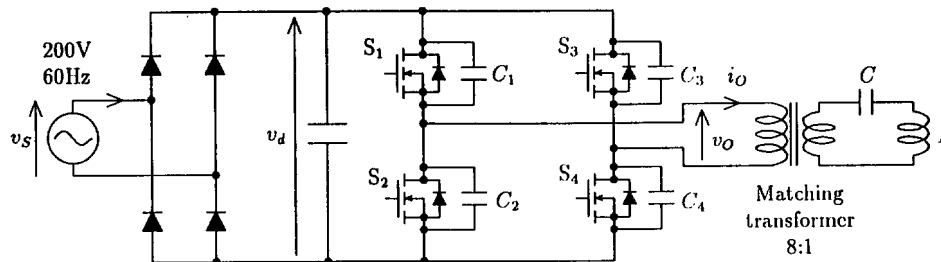Fig.2 shows three switching modes in the PDM operation. Conventional voltage-source inverters have only two
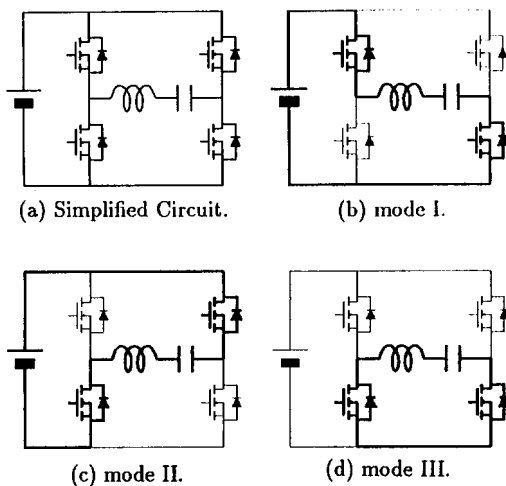
Fig.1 System configuration

(a) Simplified Circuit.　　(b) mode I.

(c) mode II.　　(d) mode III.

Fig.2 Switching modes in PDM operation

Fig.3 Switching pattern in PDM operation

switching modes such as modes I and II, while the pulse density modulated inverter additionally has mode III, in which the output voltage of the inverter is zero. If the quality factor of the resonant circuit is high enough, the resonant current continues flowing through a low side MOS-FET in one leg and a low side free wheeling diode in another leg, as discussed in the following analysis.

Fig.3 shows a switching pattern of the PDM operation. The inverter acts as a square wave voltage source for three resonant cycles, while it acts as a zero voltage source for one cycle. Therefore, the output voltage of the inverter is a periodic waveform if attention is paid to four resonant cycles. The average output voltage of the inverter is 3/4, compared with full-power operation. Thus, the output p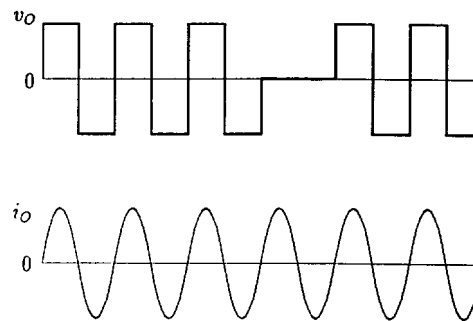ower of the inverter can be controlled by adjusting the pulse density of square wave voltage. In Fig.3, modes I and II are outputted not to include any dc component in the output voltage. As a result, no flux saturation occurs in the matching transformer. Compared with frequency control operation, the PDM operation can greatly reduce the switching losses because the MOSFET is always turned on and off at zero current.

B. Analysis of output power

Fig.4 shows specially described waveforms of output voltage and current under the assumption that the quality factor of the resonant circuit is finite. Here, a period of time of the PDM pattern, T is long enough to make the amplitude of the resonant current fluctuate. The envelope of the resonant current exhibits a first-order response although the series resonant circuit is a second-order system. The time constant of the envelope is given by

$$\tau = \frac{2L}{r} = \frac{2Q}{\omega}, \tag{1}$$

r: resistance of the resonant circuit,
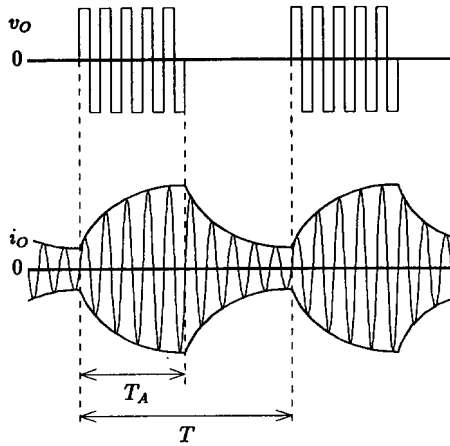Q: quality factor of the resonant circuit.

Fig.4 Voltage and current waveforms in PDM operation

The envelope i_E of the resonant current is given by

$$i_E(t) = I_m \left(1 - e^{-\frac{t}{\tau}}\right) + I e^{-\frac{t}{\tau}} \quad (0 \leq t \leq T_A)$$

$$i_E(t) = i_1(T_A) e^{-\frac{t-T_A}{\tau}} \quad (T_A \leq t \leq T) \tag{2}$$

$$I = I_m \frac{1 - e^{-\frac{T_A}{\tau}}}{1 - e^{-\frac{T}{\tau}}}, \tag{3}$$

I_m: maximum current in full-power operation,

I: initial value of the envelope i_E.

If Q is infinite, the amplitude of the resonant current is in proportion to the pulse density.

$$\lim_{\tau \to \infty} i_E = I_m \frac{T_A}{T} \tag{4}$$

The average output power is obtained by multiplying V_d and i_E, as follows:

$$P = \frac{1}{T} \int_0^{T_A} \frac{2}{\pi} V_d i_E(t) \, dt \tag{5}$$

$$= \frac{2}{\pi} V_d I_m \frac{T_A + \tau e^{-\frac{T_A}{\tau}} - \tau}{T}$$

$$+ \frac{2}{\pi} V_d I_m \frac{\tau}{T} \frac{e^{\frac{T_A}{\tau}} - 1}{e^{\frac{T}{\tau}} - 1} \left(1 - e^{-\frac{T_A}{\tau}}\right). \tag{6}$$

If the periodic time T of the PDM operation is much smaller than the time constant τ, the amplitude of the resonant current is in proportion to the pulse density, and no fluctuation occurs in the amplitude of the resonant current. Thus, the output power is in proportion to the square of the pulse density, as given by
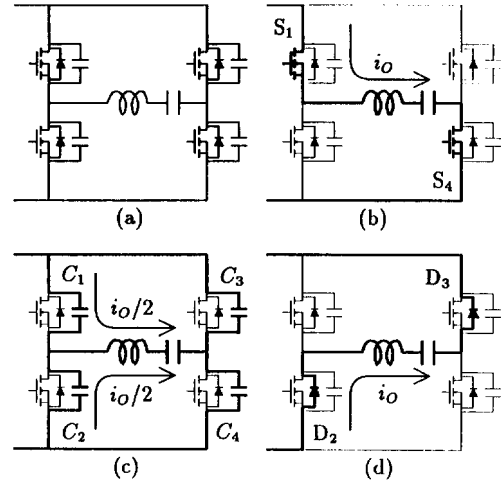

Fig.5 Principle of loss-less snubber

$$\lim_{\tau \to \infty} P = \frac{2}{\pi} V_d I_m \left(\frac{T_A}{T}\right)^2. \tag{7}$$

If $T \gg \tau$, the output power is in proportion to the pulse density because the resonant current becomes a discontinuous waveform.

$$\lim_{\tau \to 0} P = \frac{2}{\pi} V_d I_m \frac{T_A}{T} \tag{8}$$

IV. Loss-Less Snubber Circuit

A. Principle of snubber circuit

Fig.5 shows the principle of a loss-less snubber applied to the inverter. It is connected in parallel with the MOSFET in each leg, consisting of only one capacitor without any additional diode or resistor. Let's consider the switching operation from Fig.5(b), where the MOSFET's S_1 and S_4 are conducting, to Fig.5(d), where S_2 and S_3 are conducting.

First, it is assumed that the resonant current is flowing through S_1 and S_4 as shown in Fig.5(b). The voltages across the snubber capacitors C_1 and C_4 are zero, and those across C_2 and C_3 are the same as the dc link voltage. S_1 and S_4 can be turned off with zero voltage switching the instant that the gate pulses are removed from S_1 and S_4. During the commutation shown in Fig.5(c), the capacitors C_1 and C_4 are being charged, while C_2 and C_3 are being discharged with rising up of the voltages across C_1 and C_4. Since the snubber capacitors have the same capacity, half of the resonant current flows through the upper snubber capacitors and the other flows through the lower ones.
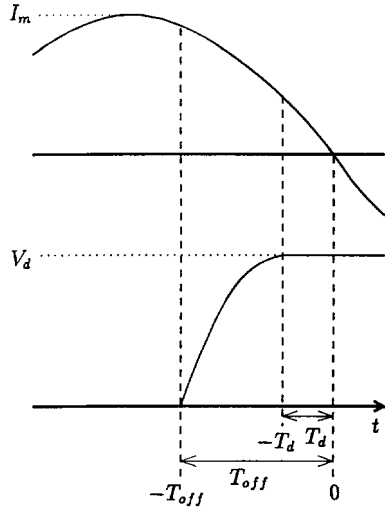
Fig.6 Waveforms of loss-less snubber circuit

When the voltages across C_2 and C_3 reach to zero, the free wheeling diodes D_2 and D_3 start to conduct as shown in Fig.5(d). S_2 and S_3 are provided with the gate pulse before D_2 and D_3 turn off. S_2 and S_3 can be turned on with zero voltage immediately the direction of the resonant current changes.

If the inverter were operated with leading power factor, this loss-less snubber circuit would not work well. It should be noted that the voltage-source inverter, in which this snubber circuit is installed, has to be operated with lagging power factor.

B. Discussion on blanking time

Fig.6 shows detailed waveforms of voltage and current of the loss-less snubber circuit. Here, assume the resonant current as follows:

$$i_O = -\sqrt{2}I \sin \omega t. \qquad (9)$$

When a MOSFET is turned off at the time of $-T_{off}$, the voltage v across the snubber capacitor starts to rise, as given by

$$
\begin{aligned}
v(t) &= \frac{1}{C_S} \int_{-T_{off}}^{t} \frac{i_O}{2} dt \\
&= \frac{I}{\sqrt{2}\omega C_S}(\cos \omega T_{off} - \cos \omega t). \qquad (10)
\end{aligned}
$$

C_S: capacitance of snubber capacitor

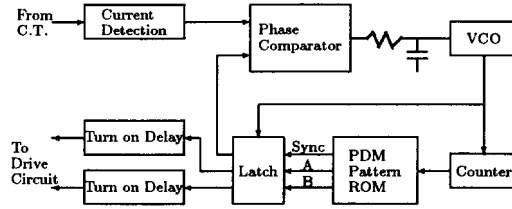The time of $-T_d$, at which the v reaches to the dc link

Fig.7 Control Circuit

voltage of V_d, is obtained by substituting into Eq.10 that $v(-T_d) = V_d$.

$$T_d = \frac{1}{\omega} \cos^{-1} \left(\cos \omega T_{off} - \sqrt{2}\omega C_S \frac{V_d}{I} \right) \qquad (11)$$

The condition that v reaches to V_d at $t = 0$ gives the minimum value of T_{off} as follows:

$$T_{min} = \frac{1}{\omega} \cos^{-1} \left(1 - \sqrt{2}\omega C_S \frac{V_d}{I} \right). \qquad (12)$$

Although Eq.12 shows an ideal condition that gives the minimum value of dv/dt, T_{off} should be set up to T_{min} for minimum pulse density because the amplitude of the resonant current is varied by pulse density. For the design of the experimental system, the minimum resonant current of 15A, which is equal to 3/4 of the rated current, and the dc link voltage $V_d = 200$V are assumed. The capacitance of the snubber capacitor is designed to be 2000pF, which is as large as the output capacitance of the MOSFET used here. Since $T_{min} = 180$ns is obtained from Eq.12, T_{off} is set up as $T_{off} =200$ns for the experimental system. The blanking time or lock-out time is also set as 150ns, because $T_d =85$ns is given by Eq.11.

V. CONTROL CIRCUIT

Fig.7 shows a control circuit of the pulse density modulated inverter. The control circuit forms a type of phase locked loop, which outputs the gate pulses in phase with the resonant current. The VCO outputs a pulse train whose frequency is twice as high as the resonant frequency. The pulse train is inputted to the five-bits step-up counter to read out a PDM pattern stored in a ROM. The PDM pattern is equal to sixteen times as long as the resonant period. Three latches inserted at the output of the ROM eliminate the effect of a delay produced by the counter and the ROM. The signal SYNC from the ROM is a continuous pulse train, and is used to synchronize the gate pulses with the resonant current. The PDM pattern signals A and B are inputted to a set-up circuit of blanking time and then are provided to a drive circuit.
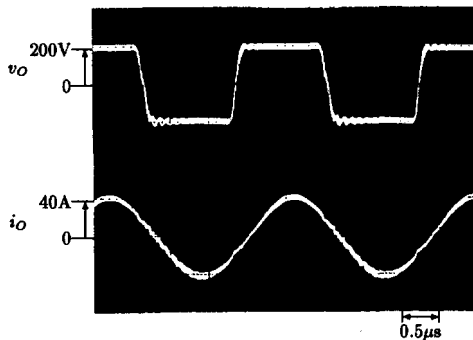
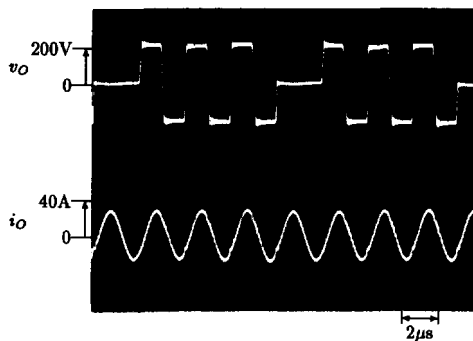Fig.8 Experimental waveforms of inverter output (full-power operation).

Fig.9 Experimental waveforms of inverter output (pulse density: 3/4).
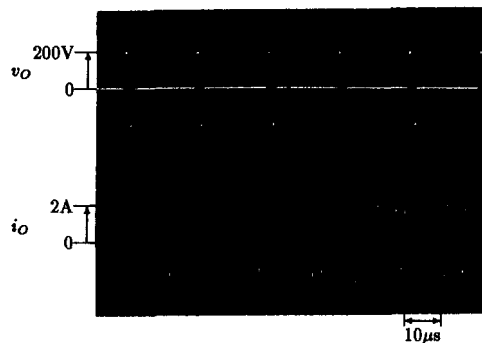

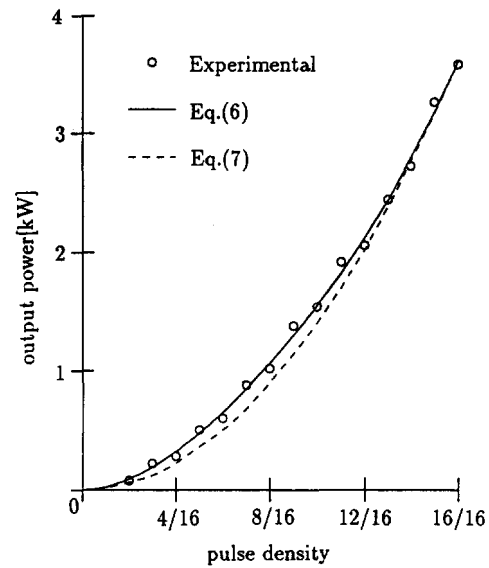Fig.10 Experimental waveforms of inverter output (pulse density: 1/8).

Fig.11 Relationship between pulse density and output power.

VI. EXPERIMENTAL RESULTS

Figs.8, 9 and 10 show experimental waveforms obtained by a prototype system. In these experiments, a dielectric capacitor of $3000\mu F$ is connected with the dc link to verify the operation principle of pulse density modulation.

Fig.8 shows an output voltage and current of the high-frequency inverter in the case of the full-power operation of about 3.6kW. Since the snubber capacitor of 2000pF suppresses dv/dt, that is, the derivative of the drain to source voltage with respect to time, the rise-time is about 150ns. No voltage spike occurs in the output voltage.

Figs.9 and 10 show those in the case of the PDM operation. Since the pulse density is equal to 3/4 in Fig.9, the amplitude of i_O decreases according to the pulse density. Almost no decay caused by the PDM operation appears in the amplitude of i_O. In Fig.10, the amplitude of i_O is greatly reduced by the PDM operation, and the output power of the inverter is 80W, which is only 2%, compared with that in Fig.8. The periodic time of the PDM operation in Fig.10 is longer than that in Fig.9, so that the amplitude of i_O fluctuates.

Fig.11 indicates a relationship between the pulse density and the output power of the inverter. The curve obtained from Eq.6 agrees well with the experimental results. The curve given by Eq.7 has a small difference in the range of pulse density from 2/16 to 12/16. This means that Eq.7 is
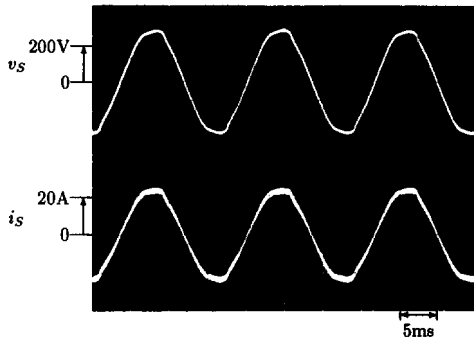
Fig.12 Experimental waveforms in case of using diode rectifier without dielectric capacitor (full-power operation).
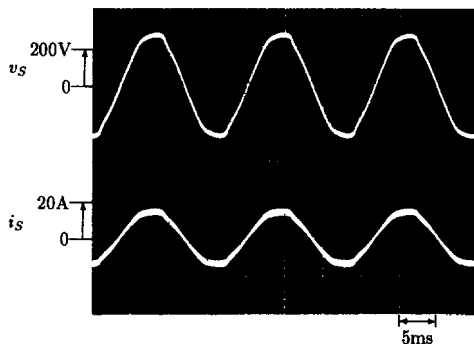

Fig.13 Experimental waveforms in case of using diode rectifier without dielectric capacitor (pulse density: 3/4).

applicable in the range of output power from 70% to 100%, while Eq.6 is valid in the overall range.

Fig.12 shows the waveforms of the input voltage and current of the diode rectifier in the case of the full-power operation. The input current is a sinusoidal waveform with unity power factor, because no dc capacitor is connected to the diode rectifier except for a high frequency capacitor of 0.47μF. Fig.13 shows those in the case of pulse density=3/4. Although the pulse density modulated inverter produces the current ripple, the frequency of which is about 100kHz, the ripple can be absorbed by the high frequency capacitor.

VII. CONCLUSION

The purpose of this paper is to develop a pulse density modulated inverter of 4kW 400kHz which can be used as an induction heater in a dental casting machine. Since the output power of the inverter is controlled by itself, a

diode bridge rectifier is applicable. The PDM control realizes zero current switching in all the operating conditions so that it can reduce switching losses and electromagnetic noises, compared with frequency control or PWM control. This results not only in improving efficiency but also in reducing volume or size of induction heating systems. It is believed that the pulse density modulated inverter is more suitable for induction heating systems from a practical point of view.

REFERENCES

[1] W. E. Frank, C. F. Der, "Solid State RF Generators for Induction Heating Applications," IEEE/IAS Annual Meeting, pp.939-944, 1982.

[2] S. Bottari, L. Malesani, P. Tenti, "High Frequency 200kHz Inverter for Induction Heating Applications," IEEE/PESC Rec., pp.308-316, 1985.

[3] H. Akagi, T. Sawae, A. Nabae, "130kHz 7.5kW Current Source Inverters Using Static Induction Transistors for Induction Heating Applications," IEEE Trans. on Power Electronics, Vol.PE-3, No.3, pp.303-309, 1988.

[4] T. Yokoo, H. Itho, A. Sano: "High Frequency Inverter for Induction Heating Equipment by Using Static Induction Transistor," PCIM Proc., pp.101-108, 1988.

[5] P. P. Roy, S. R. Doradla, S. Deb: "Analysis of the Series Resonant Converter Using a Frequency Domain Model," IEEE/PESC Rec., pp.482-489, 1991.

[6] A. Dmowski, R. Bugyi, P. Szewczyk: "A Novel Series-Resonant DC/DC Converter with Full Control of Output Voltage at No-Load Condition. Computer Simulation Based Design aspects," IEEE/IAS Annual Meeting, pp.924-928, 1992.

[7] M. Nakaoka, Y. J. Kim, H. Ogiwara, H. Uemura: "Modern Digitally-Controlled Constant High-Frequency PWM Resonant DC-DC Converter Using Lumped Parastic Reactive Circuit Components of High-Voltage Transformer & Feeding Cable and its New Practical Application," IEEE/IAS Annual Meeting, pp.1088-1097, 1991.

[8] W. H. Kwon, G. H. Cho: "Modified Quantum and Phase Control of Series Resonant Converter," IEEE/PESC Rec., pp.498-503, 1991.